Common structural features of different viroids: serial arrangement of double helical sections and internal loops

Jörg Langowski[+] , Karsten Henco, Detlev Riesner*, and Heinz Ludwig Sänger**

Institut für Organische Chemie und Biochemie, Technische Hochschule, Petersenstr. 22, D 6100 Darmstadt, and Institut für Klinische Biochemie und Physiologische Chemie, Medizinische Hochschule Hannover, GFR

ABSTRACT

The thermodynamic parameters of five different highly puri-
fied viroid "species" were determined by applying UV-absorption
melting analysis and temperature jump methods. Their thermal de-
naturation proved to be a highly cooperative process with mid-
point-temperatures (T_m) between 48.5 and 51°C in 0.01 M sodium
cacodylate, 1 mM EDTA, pH 6.8. The values of the apparent reac-
tion enthalpies of the different viroid species range between
3,140 and 3,770 kJ/mol. Although the cooperativity is as high as
found in homogeneous RNA double helices the T_m-value of viroid
melting is more than 30°C lower than in the homogeneous RNA. In
order to explain this deviation, melting curves were simulated
for different models of the secondary structure of viroids using
literature values of the thermodynamic parameters of nucleic
acids. Our calculations show that the following refinement of
our earlier model is in complete accordance with the experimental
data: In their native conformation viroids exist as an extended
rodlike structure characterized by a series of double helical
sections and internal loops. In the different viroid species
250-300 nucleotides out of total 350 nucleotides are needed to
interpret the thermodynamic behaviour.

INTRODUCTION

There has been an increasing interest in viroids because it
is known that they are the smallest infectious and pathogenic en-
tities in nature found to date (see Review by T.O. Diener [1]).
They are coat protein-free RNA molecules of a molecular weight
of 120,000 daltons and cause several economically important dis-
eases in higher plants. Little is known about their mechanism of
replication and pathogenicity; their genetic information is not
sufficient to code for a protein with a molecular weight larger
than 10,000 if they were translated. The availability of suffi-
cient amounts of purified viroid material of electrophoretic ho-
mogeneity for optical absorption studies has led to several bio-
chemical and physico-chemical investigations of their molecular

structure [2-5]. It has been shown that viroids are single-
stranded, covalently linked, circular RNA molecules. They are
the first such RNA natural occurring structures ever discovered
in nature [2]. Under native conditions viroids exist in a highly
base-paired rod-like conformation. Thermodynamic and kinetic
studies on CPFV [6] gave further insight into the secondary
structure of viroids [4]. The thermal denaturation process
proved to be highly cooperative with the half width of the
melting curves between 1-3°C. It could be resolved by kinetic
techniques into two processes, a dominant process in the time
range of sec and a minor contribution in the msec range. The
slower denaturation process had been interpreted in terms of an
all-or-none opening of a fairly homogeneous intramolecular
double helix of 50-60 base pairs, whereas the faster process
had been taken as an indication for the existence of additional
shorter hairpin branches.

In this paper we present a systematic comparison of five
different viroid species and give a statistical thermodynamic
description of their denaturation. In contrast to the previous
study our present calculations do not rely on the limited valid-
ity of the all-or-none approximation in which only the native
and the fully denatured states were taken into account. Whereas
the earlier model was based on enthalpies only, we describe in
this paper a refined model, which is in accordance with both,
the measured T_m values as well as the measured enthalpies. The
correspondence of the thermodynamic evaluation given in this
work with calorimetric studies of an accompanying paper [7] will
be discussed.

MATERIALS
The origin, propagation and purification of CEV, PSTV,
ChSTV, and CPFV [6] was as previously described [2,5,8]. The
original culture of ChCMV [6] was kindly provided by Dr. M. Hol-
lings, Littlehampton, and this viroid was propagated in the
Chrysanthemum morifolium cultivar "Yellow Delaware". Precautions
were taken to prevent any cross-contamination between these
viroids. Their purity and individual characteristics were rou-
tineley checked by fingerprinting [5].
Samples have been used without further dialysis. All expe-

riments were carried out in a standard buffer containing 0.01 M sodium cacodylate,1 mM EDTA, pH 6.8 and NaCl as specified in the text. All chemicals were of analytical grade and triple distilled water was used. All samples were heated to 60-70°C prior to the experiment to exclude metastable conformations.

METHODS

Melting curves and slow temperature-jumps were carried out in a thermostatable cuvette which was especially constructed for fast temperature changes and small volumes as described elsewhere ([4]; Henco and Riesner, to be published). Temperature equilibration was achieved in less than 1 sec; the volume is 70 µl with an optical path length of 2 cm. For fast temperature-jumps the Eigen-DeMaeyer technique was used. The particular design of our instrument was described in detail in [9]. Computer calculations were performed on a Cyber 76 and a Prime 300.

THEORY

The theoretical treatment of the thermodynamic behaviour of viroids is based on the elementary thermodynamic parameters common to all ribonucleic acids. These parameters are used in partition functions particularly adapted to viroids. This again is combined with the hypochromicity to simulate the experimental melting curves. Of these three, it is mainly the partition function which reflects the particular properties of the models for the secondary structure.

1. Elementary thermodynamic parameters

Chain growth

The equilibrium constant s is assigned to the reaction of forming an intact base pair next to one intact pair with:

$$-RT \ln s = \Delta G_{bp} = \Delta H_{bp} - T \, \Delta S_{bp} \qquad (1)$$

where R is the gas constant, T the absolute temperature, and ΔH_{bp} and ΔS_{bp} the changes in enthalpy and entropy, respectively.

Borer et al. [11] and Gralla and Crothers [12] determined those parameters for all possible sequences of two adjacent base pairs. Their values for ΔH_{bp} and ΔS_{bp} are temperature independent constants determined below 50°C. Pörschke et al. [13] did not regard particular nucleotide sequence effects, but included a tempera-

ture dependence of the ΔH-values via a coupled stacking-un-
stacking equilibrium of the dissociated single strands. Two
terms of the free energy, ΔG_K for base pairing from the com-
pletely coiled state and ΔG_A for single strand stacking con-
tribute to the effective free energy ΔG_{eff} for base pairing
according to:

$$\Delta G_{eff} = \Delta G_K - F \cdot RT \ln (1 - \exp(\Delta G_A/RT)) \qquad (2)$$

with F = 1 for $\genfrac{}{}{0pt}{}{A}{U}$ $\genfrac{}{}{0pt}{}{A}{U}$ interactions, since UU is the only sequence
without major stacking, and F = 2 for all other sequences.

Since only the AU/GC content but not the nucleotide se-
quences of viroids are known it is not possible at present to
take advantage of the data including sequence effects. The tem-
perature dependence of the model data, however, may be important,
since those data will be applied to processes occurring near
80°C, but have been determined at much lower temperatures. Com-
parison of theoretical and experimental T_m-values of double-
stranded polymeric RNA's (cf. [14]) agree with one another, if
we use the parameters of Pörschke et al. or Gralla and Crothers,
whereas the data of Borer et al. led to higher melting points.
Throughout this work the data of Pörschke et al. were used.

Hairpin loop formation

The equilibrium constant for the formation of an isolated
base pair leaving p bases unpaired in a loop is defined as:
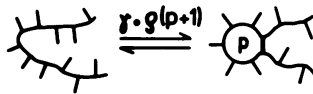
The factor γ is an intrinsic constant for base pairing which is
independent of the loop geometry, whereas the so called loop
weighting f·.action ρ(p + 1) denotes the concentration of one
base relative to the (p + 1) next base. A value of γ = 0.003
has been reported by Elson et al. [15] . For loops larger than
14 nucleotides the Jacobson-Stockmayer-approximation [16]:
$\rho(p + 1) = 0.319 \cdot p^{-3/2}$ with the factor 0.319 from [17] has been
applied to our problem and for loops smaller than 14 the results

from Monte-Carlo-treatment of nucleotide chain geometry [18,19] were used.

Internal loop formation

Internal loops are unpaired regions between two double helical regions:
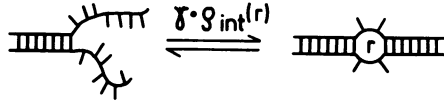
Gralla and Crothers [20] reported values for internal loops of 2-8 unpaired bases. For larger internal loops the data of hairpin loops will be used.

Average parameters

The equilibrium constant K for double helix formation of k base pairs is:

$$K = \gamma \rho (p + 1) \prod_{i=2}^{k} s_i , \qquad (3)$$

with the growth parameter for the i_{th} base pair s_i which is different for AU and GC pairs. Since viroid sequences are not known, we use the average growth parameters dependent upon the AU/GC content with:

$$\prod_{i=2}^{k} s_i = s^{k-1} \qquad (4)$$

The averaging of Eq. (4) holds only for random sequences which lead to fairly homogeneous transitions as experimentally found (cf. Fig.1). If, in contrast, AU and GC pairs were present in large clusters, different peaks in the melting curves would be expected and the use of average parameters would not be acceptable.

Average values of ΔH_{bp} and ΔS_{bp} follow from Eq. (4):

$$\Delta H_{bp} = (1 - f_{GC}) \cdot \Delta H_{AU} + f_{GC} \cdot \Delta H_{GC}$$
$$\Delta S_{bp} = (1 - f_{GC}) \cdot \Delta S_{AU} + f_{GC} \cdot \Delta S_{GC}, \qquad (5)$$

if f_{GC} is the fraction of GC pairs. The correction factor F (cf. Eq. (2)) was derived as above:

$$F = 1.5 + f_{GC}(1 - 0.5 \, f_{GC}). \qquad (6)$$
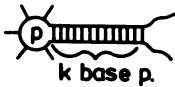
2. Partition function

It is essential for our conclusions to proceed stepwise

from very approximative to more general models, and to check
which type of refinements leads to an acceptable fit to the ex-
perimental results.

One helical section model

Only one uninterrupted double helical section exists dur-
ing the transitional states in the whole molecule. The partition
function will be given in parallel for hairpin structures origi-
nating from linear chains and for dumb-bell structures which
originate from closed circles. States of the following type are
considered:

hairpin

k base p.

with:

$$p_{min} \leq p \leq (p_{min}+2(k_{max}-1))$$

$$1 \leq k \leq k_{max}$$

dumb-bell

k base p.

and:

$$p_{min} \leq p \leq (p_{min}+2(k_{max}-1))$$

$$q = l_{tot} - 2k - p$$

$$1 \leq k \leq k_{max} \tag{7}$$

$$l_{tot} : \text{total number of nucleotides}$$

The native state is characterized by p_{min}, q_{min}, and k_{max}. The
statistical weight of any given state for the hairpin is:

$$P_{1,hp}(p,k) = \rho(p+1) \cdot s^{k-1}, \tag{8}$$

and according to Scheffler et.al. [21] for the dumb-bell:

$$P_{1,db}(p,l_{tot},k) = \gamma \cdot \frac{\rho(p+1) \cdot \rho(q+1)}{\rho(l_{tot})} \cdot s^{k-1}. \tag{9}$$

The first index of p denotes the number of helical sections tak-
en into account. Base pairing schemes which deviate from the
scheme of the native viroid have not been taken into account be-
cause of the very low thermodynamic probability.

The partition functions are given in Eq. (10) and Eq. (11).
In a particular intermediate j base pairs are dissociated on
the left side of k intact base pairs and are included in the
left side loop of $p_{min}+2j$ bases.

$$z_{1,hp} = 1 + \sum_{k=1}^{k_{max}} \sum_{j=0}^{k_{max}-k} P_{1,hp}(p_{min}+2j,k), \tag{10}$$

and for dumb-bells:

$$Z_{1,db} = 1 + \sum_{k=1}^{k_{max}} \sum_{j=0}^{k_{max}-k} P_{1,db}(p_{min}+2j, l_{tot}, k).$$ (11)

Models with two, three, and four helical sections

A more general model containing internal loops or helical defects is considered. These internal loops are in the native state due to the nucleotide sequence of the molecule. All helices are in a linear arrangement and extensive branching as in tRNA or MS2 does not occur. Branching would result in much lower cooperativity than observed in viroids which follows from a comparison of experimental [10] and theoretical [14] results of tRNA. Furthermore a highly extended structure of viroids was deduced from electron microscopy and hydrodynamic studies on viroids [2]. Structures of the following type are discussed:
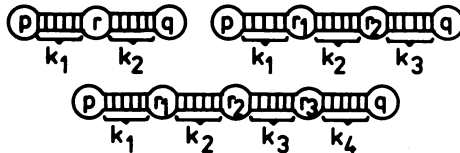
The thermodynamic probability for two helical sequences $P_{2,db}$ (for dumb-bell) contains an additional nucleation step due to the internal loop:

$$P_{1,db}(p, r, l_{tot}, k_1, k_2) = \gamma^2 \frac{\rho(p+1)\rho(q+1)}{\rho(l_{tot})} \rho_{int}(r) \cdot s^{k_1+k_2-2}$$ (12)

with $q = l_{tot} - 2k_1 - 2k_2 - p - r$. States with one helical section are taken into account as intermediates. The partition function is obtained by summation over all states with either $k_1 = k_2 = 0$ (completely coiled state), $k_1 = 0$, and $k_2 \neq 0$ (first helical section completely unpaired), $k_1 \neq 0$ and $k_2 = 0$ (second helical section completely unpaired), and $k_1 \neq 0$ and $k_2 \neq 0$ (both helical sections partially or completely paired).

An equivalent summation procedure is also applied for more than two helical sections. The statistical weight for a state

with m helical sections is:

$$P_{m,db}(p, r_1, \ldots r_{m-1}, l_{tot}, k_1, \ldots, k_m)$$

$$= \gamma^m \frac{\rho(p+1) \cdot \rho(q+1)}{\rho(l_{tot})} \cdot \prod_{j=1}^{m-1} \rho_{int}(r_j) \quad \prod_{i=1}^{m} s^{k_i - 1} \tag{13}$$

Partition functions up to four helical sections have been calculated by this method. Models with more helical sections consume too much computer time and have been treated by approximation in the next paragraph.

Multiple all-or-none model (MAN)

If the size of the helical section is sufficiently small, i. e. less than 10 base pairs, one may assume, that during the transition every single helical section is either completely dissociated or fully base paired [10]. The approximation of such a multiple all-or-none model leads to a drastic reduction in the number of possible intermediate states. All helical sections are identical, i. e. the type and frequency of internal loops are averaged in an equivalent way as elementary parameters.

For a simple derivation of the partition function a binary value I with a number of bits equal to the number of helical sections in the molecule is assigned to each defined state. A value of 1 in the nth bit means that the nth helical section is closed, value 0 for the open state, respectively. The statistical weight $P_{MAN,db}(I)$ for a given binary number was calculated according to a simple algorithm [22]. The partition function is:

$$Z_{MAN,db} = \sum_{\text{all binary values } (I)} P_{MAN,db}(I) \tag{14}$$

3. Simulation of melting curves

Degree of transition and hypochromicity

The degree of transition $\Theta(T)$:

$$\Theta(T) = \frac{\text{average number of base pairs present at T}}{\text{number of base pairs in the native state}}$$

is followed experimentally via the hypochromicity. The hypochromicity/base pair (hy) depends not only upon the type of base pair but also upon the number of base pairs k in the corresponding helical section. We have included the dependence on k by inter-

polating literature values of $hy(k)$ of different oligonucleo-
tides [29,30] according to:

$$hy(k) = hy(\infty) \; (1 - 0.4/k) \tag{15}$$

The relative hypochromicity $Hy(T)$ is obtained from $\theta(T)$ by
weighting each double helical section of k_i base pairs with the
hypochromicity $hy(k_i)$:

$$Hy(T) = \frac{\displaystyle\sum_{\text{all states}} p(p, r_1 \ldots r_{m-1}, l_{tot}, k_1, \ldots, k_m) \sum_{i=1}^{m} k_i \, hy(k_i)}{Z \cdot \displaystyle\sum_{i=1}^{m} k_{i,max} \cdot hy(k_{i,max})}$$

$$= \frac{A(T) - A(T_o)}{A(T_1) - A(T_o)} \tag{16}$$

with the optical absorption $A(T)$, and T_o and T_1 random tempera-
tures below and above the range of transition, respectively.

Cooperativity

The cooperativity is a measure of the validity of the all-
or-none model. If the helix-coil transition of the whole mole-
cule is evaluated in terms of a single all-or-none transition,
one obtains an apparent reaction enthalpy ΔH_{app} according to [10]:

$$\Delta H_{app} = 4 \; RTm^2 \cdot \frac{d\theta}{dT}\Big|_{T_m} \tag{17}$$

with $\dfrac{d\theta}{dT}\Big|_{T_m} = \dfrac{dHy}{dT}\Big|_{T_m}$.

Dividing ΔH_{app} by ΔH_{bp} (cf. Eq. (5)) and adding 1 for the
nucleation yield k_{coop}, the number of base pairs opening in an
all-or-none process:

$$k_{coop} = 1 + \Delta H_{app}/\Delta H_{bp} \tag{18}$$

The cooperativity is defined as k_{coop}/k_{max}, or if k_{max} base
pairs are present in m helical sections and the first base pair
of each helical section does not contribute to ΔH.

$$\text{cooperativity} = (m + \Delta H_{app}/\Delta H_{bp})/k_{max} \tag{19}$$

RESULTS

I. Experiments

1.) Melting curves in low ionic strength

The melting curves of five different viroids as determined
in 0.01 M sodium cacodylate, 1 mM EDTA, pH 6.8 are shown as dif-
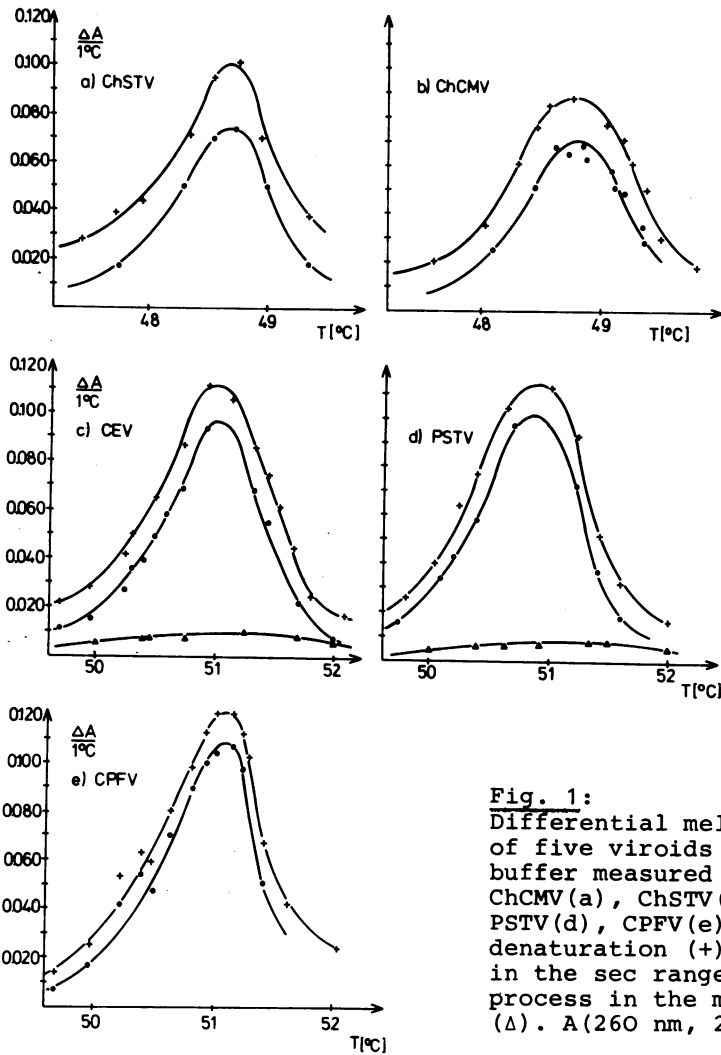ferential melting curves in Fig. 1. They are characterized by a

Fig. 1:
Differential melting curves of five viroids in standard buffer measured at 260 nm: ChCMV(a), ChSTV(b), CEV(c), PSTV(d), CPFV(e). Total denaturation (+), process in the sec range (o), process in the msec range (Δ). A(260 nm, 20°C) = 1.

very narrow temperature range of the transition which is common to all viroid species.

The model calculations show (v. i.) that this type of melting curve is characteristic for a highly cooperative melting process involving many base pairs. It differs strikingly from the melting of tRNA e. g., which ranges over more than 20°C under identical conditions. To rule out the possibility that the differences in T_m (Table 2) are due to inaccuracies in the ionic strength of the solutions CEV and CSTV [6] were mixed and their melting processes were studied in the mixture. Fig. 2 demonstrat-
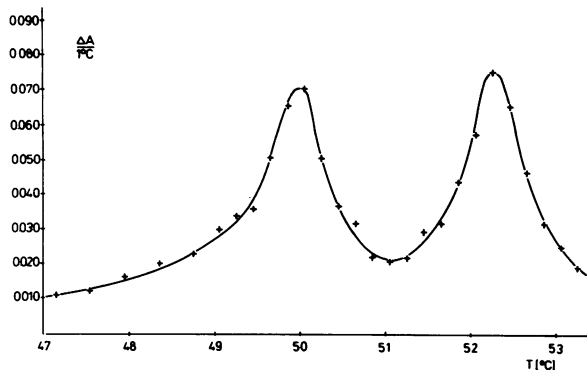
Fig. 2:
Differential melting
curve of a mixture
of 49% ChSTV and 51%
CEV in 0.012 M sodium
cacodylate, 1 mM EDTA,
pH 6.8. A(260 nm,
$20^{\circ}C$) = 1.06.

es that the melting peaks of both viroid species are clearly sep-
arated and that their T_m values are identical to those determined
individually.

2.) Separation of base pairing and single strand stacking

The kinetics of the melting processes were measured as pre-
viously reported for CPFV [4]. In the present study only the re-
laxation amplitudes are used for the evaluation and a forthcom-
ing paper will deal with the relaxation times. The total relax-
ation effect could be resolved into a homogeneous, slow process
in the time range of seconds, which is the main contribution of
the total hypochromicity, and into a fast process in the msec
range with a smaller amplitude. The latter was systematically
studied only in CEV and PSTV. Although the faster process could
not always be characterized by a single relaxation time it was
clearly separated from the slow process. Beside these two well
resolved processes a third process faster than the instrumental
time constant was detected. This process represents only a small
contribution of the total hypochromicity in the temperature range
of the transition. It is due to the stacking-destacking equilib-
rium of single stranded regions, and it is observed in the dena-
turation of all nucleic acids (cf. [10]). Because we were only
interested in base pairing, only the sum of the resolved process-
es were used for the quantitative interpretation.

In Table 2 the apparent reaction enthalpies ΔH_{app} are listed
which were derived from the sum of the resolved processes using
standard procedures (Eq. (17)). At present, it cannot be clari-
fied why the halfwidth measured on CPFV is smaller than the value

determined on an earlier preparation of CPFV [4]. The GC-content
of the base pairs melting in the denaturation process was deter-
mined from the wavelength dependence of the hypochromicity [4].
The data on T_m, ΔH_{app} and the GC-content are the basis for the
theoretical treatment.

3.) Ionic strength dependence of the T_m-value and the half-width
    of transition

     Fig. 3 shows the dependence of the T_m-value upon the ionic
strength. The dependence is nearly linear between 0.005 M and
1 M NaCl with a slope of 13.2°C/log $c_{Na}+$. In 1 M NaCl the T_m val-
ue is of particular interest, because the theoretical thermody-
namical treatment refers to this high ionic strength at which
electrostatic interactions may be neglected and for which the
thermodynamic parameters are known from the literature.

     The widths of the transition in low and high ionic strength
are identical within the limits of error which was experimentally
verified on CPFV. For experimental reasons, the detailed studies
on the shape of the transition curves of the other viroids in-
cluding the kinetic analysis, were only carried out in lower ion-
ic strength. For the theoretical part of this study it is assumed
that the shape of the melting curves for all of the other viroids
are similarly independent upon the ionic strength as observed
for CPFV.

II. Estimation_of_secondary_structure_through_comparison_of
    calculated_and_measured_melting_curves

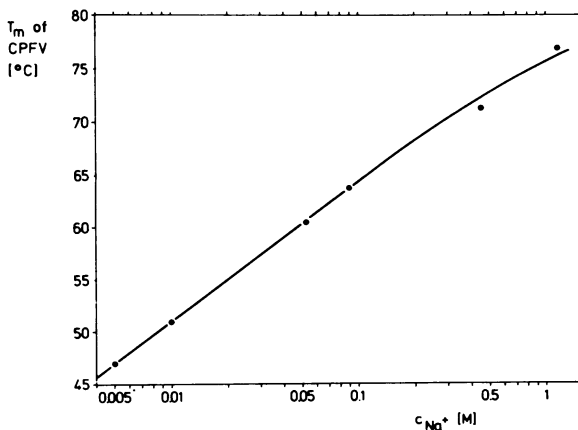   All calculations refer to 1 M ionic strength. It is assumed

Fig. 3:
Dependence of T_m of
CPFV upon the
ionic strenth (Na^+)
in standard buffer.

that electrostatic repulsion of the backbone phosphates has no specific influence under these conditions.

1.) Linear and circular strands in the one-helical-section approximation

Although the assumption of a single uninterrupted helical section is a rough approximation, some thermodynamic properties of linear strands forming hairpins and circular strands forming dumb-bells can be derived from this simplified model.

T_m-values

The dependence of the T_m-value on the number of base pairs k is shown in Fig. 4 a+b. In the first set of calculations (Fig.4a) the loop size has been kept constant and the total length of the
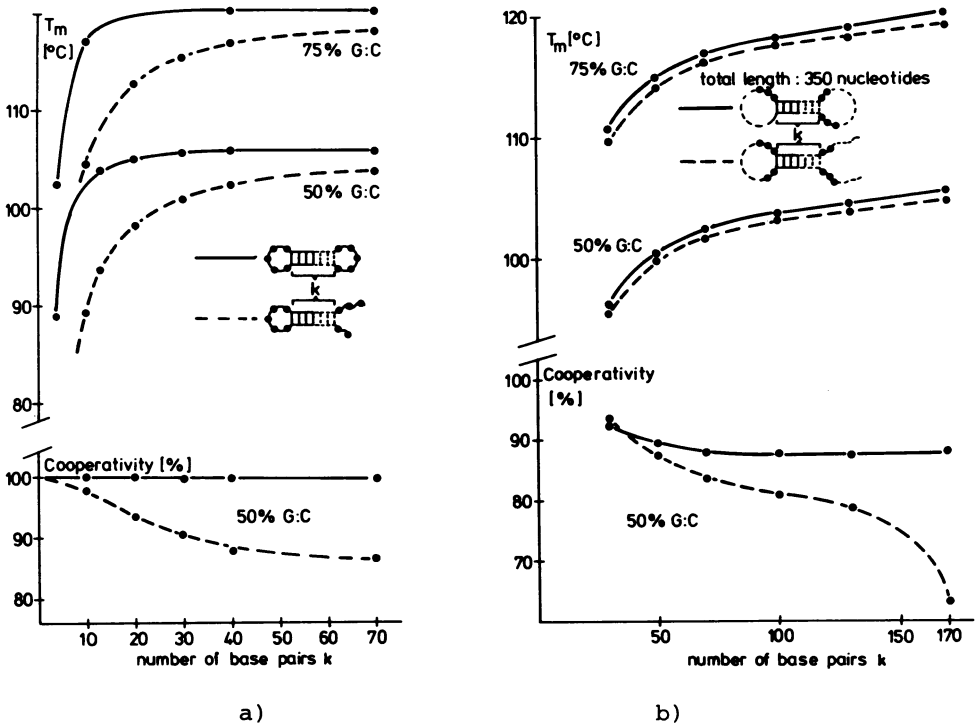

a)   b)

Fig. 4:
Calculated dependence of T_m-values and cooperativities upon the number of base pairs in the one helical sequence model.
a) constant loop size of 5 nucleotides, variable total length;
b) variable loop size, constant total length of 350 nucleotides. For easier presentation the calculated points are connected by continous functions.

molecule has been varied between 20 and 130 bases. A loop size of
5 bases, which is known to be most favourable for adjacent double
helix formation, was chosen for these calculations [18,19,21].
Variation of the G:C content does not change the shape of the
functions in Fig. 4 a+b and it only shifts all T_m-values to the
same degree. Dumb-bell structures are more stable than hairpins
and they reach their final level in the T_m-values with less base
pairs. The difference in T_m between both structures decreases
with increasing number of base pairs and is less than 2^OC for
molecules with more than 70 base pairs - the number which has
been found in viroids (v. i.).

In the second set of the model calculations (Fig. 4b) the
total length of the RNA was held constant at 350 bases - the
size of viroids. The number of base pairs k determines the loop
size. The difference in T_m between both structures is nearly
constant for all possible numbers of base pairs because the in-
creasing number of base pairs and the simultaneously decreasing
loop size have an opposite influence on the difference in T_m.

Cooperativity

Fig. 4 a+b shows the cooperativity in dependence upon the
number of base pairs. The cooperativity of dumb-bells is always
higher that that of hairpins. In the first set of model RNAs
dumb-bells show approximately 100% cooperativity up to 70 base
pairs due to the small loops. If the model RNAs are of the size
of viroids as in the second set of calculations, the cooperativ-
ity is fairly independent of the number of base pairs at a value
close to 90%. This is because the increasing number of paired
bases lowers the cooperativity, but the simultaneously decreasing
number of unpaired bases in both loops raised the cooperativity.
It follows that an evaluation in terms of an all-or-none process
could result in a good estimation of the number of base pairs in-
volved. This is a justification for such an evaluation of the
melting curves which were described in our earlier paper [4].

Discrepancy of the one-helical-section model with the experimen-
tal results

In applying the one-helical-section model, it was possible
to simulate the shape of the melting curves fairly well. 70-100
base pairs have to be assumed for the different viroids, which

would be in agreement with the measured half width between 1.4 and 0.9°C.

There is, however, a major discrepancy between the theoretical and experimental results which cannot be clarified by the assumption that one uninterrupted double helix exists. The T_m-values were calculated to 110 or 125°C (for 50 or 75% GC, respectively), whereas a T_m-value at 76°C in 1 M NaCl was determined experimentally. This discrepancy of about 35°C cannot be due to the choice of a particular set of elementary parameters (cf. "Theory"), since the use of other parameters [11,12] leads to a similar or even greater discrepancy.

2.) Influence of internal loops and helix defects

To overcome the discrepancy between measured T_m and calculated T_m, it was assumed that the double helix is not completely homogeneous but is interrupted by several internal loops or helix defects. As pointed out earlier (cf. paragraph "Theory") all helical sections were assumed to be identical and have to be regarded as an average from shorter and longer helical sections, smaller and larger loops, single unpaired bases and mismatches. The influence of such helix defects may be seen on model molecules, that are much smaller than viroids. The exact partition function according to paragraph "Theory" has been applied to circular molecules of varying size of the internal loops and the helical sections.

The results are seen in the simulated melting curves of Fig. 5. The RNA molecules of Fig. 5 have 12 nearest neighbour stacking interactions either in a homogeneous helix or with 1,2, or 3 internal loops. Two properties are evident: The T_m-value is shifted due to each additional internal loop, whereas the cooperativity is lowered mainly by the first internal loop. Therefore, it should be possible to find values of internal loop size and helix length which would be in accordance with the high cooperativity and low T_m-values found on viroids.

The extrapolation to the properties of viroids has been carried out in the following way. The size of the loops and helical segments has been kept constant, while their number was increased to the total chain length of viroids. The exact partition functions were used for molecules up to four helical sections, and
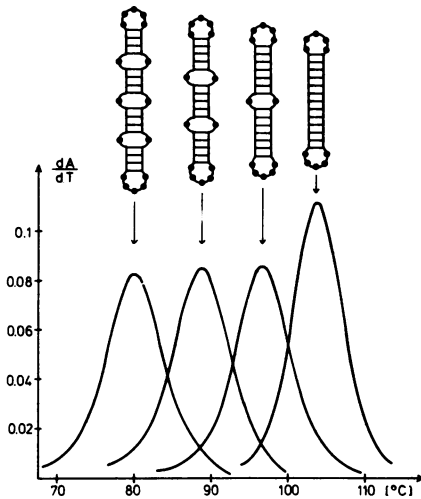
Fig. 5:
Simulated melting curves of
defective double helices as
indicated in the figure: All
molecules contain 12 nearest
neighbour interactions with
50% G:C.

molecules with more helical segments had to be treated by the
MAN-model (cf."Theory"),The results are shown in Fig. 6. The T_m-
value decreases continously with the increasing number of helical
sections. For 2,3, or 4 helical segments both methods have been
applied. The MAN-model resulted in about $2^{\circ}C$ lower T_m-values than
the exact partition function; both functions, however, are in par-
allel. Therefore, the increment in T_m with increasing number of
helical segments is correct when calculated by the MAN-model and
only the absolute numbers may be wrong by $2^{\circ}C$ due to the simpli-
fied model. We do not regard this deviation as serious because
the original discrepancy in T_m which we tried to interpret was
about $35^{\circ}C$, and furthermore, the uncertainties due to the re-
stricted accuracy of the data from model oligonucleotides are
most probably larger than $2^{\circ}C$.
The equivalent calculations carried out for 75% GC resulted in
about $15^{\circ}C$ higher T_m-values and nearly identical cooperativities.
        The influence of internal loops on the cooperativity is
small as seen from Fig. 6. The values obtained by the correct
partition function level off near 85% with increasing number of
helical sections. The cooperativity calculated by the MAN-model
is incorrectly high in small molecules. In larger molecules, as
viroids, however, the melting temperature decreases markedly due
to the many internal loops. At the lower temperatures the ratio
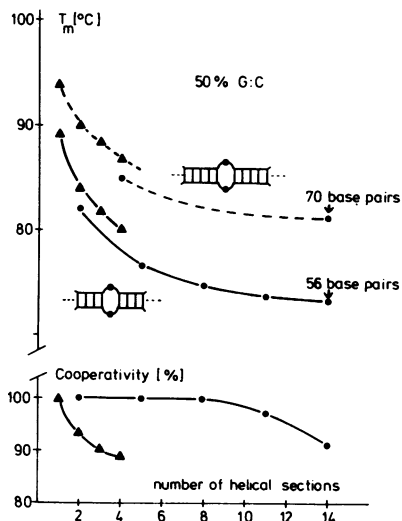of nucleation parameter/growth parameter becomes smaller, so that

Fig. 6:
Calculated dependence of the T_m-values and cooperativities upon the number of helical sections in the defective helix models. Circular molecules have been treated either by exact partition function (Δ) or by the MAN-model (o); 5 base pairs/section, two bases/internal loop (---); 4base pairs/section, two bases/internal loop (———).

the cooperativity of each helical section increases, and the MAN-model becomes more realistic.

The effect of the size of the internal loops and of the number of base pairs/helical section may be seen from the results listed in Table 1. Whereas the cooperativity is near 90%

Table 1

number of nucleotides per internal loop	number of base pairs per helical section	model (50% G:C)	T_m [°C]	Cooperativity [%]
2	4		80	88.5
2	5		87	88
2	6		91	87
4	4		76	91.5
6	4		73	91
8	4		67	90.5

in all examples, larger internal loops lower the T_m-value and longer helical sections raise the T_m-value. Therefore, one has to conclude, that a molecule with many small internal loops leads to a similar melting curve as a molecule with less but larger internal loops.
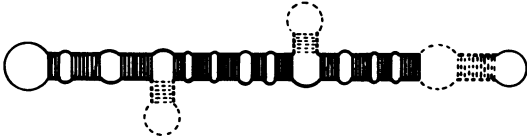
DISCUSSION

The experimental results show, that all viroids investigated to date have similar thermodynamic properties. Their T_m-values differ only within $3^\circ C$ and the cooperativity of the thermal transition is exceptionally high as compared to other single stranded RNAs [10,23,24,25]. Our calculations indicate that the high cooperativity is at least in part a consequence of their circularity. The common biological properties of viroids i. e. their infectivity and pathogenicity correspond to common structural features which are evident not only from this work, but also from hydrodynamic [2], electron microscopic [2]   and kinetic studies. Although thermodynamic differences between individual viroids are well established, we will mainly discuss the properties which are common to all viroids. The differences can only be related to the individual nucleotide sequences, which are not available as yet.

1. Defective helix model

The earlier model of a nearly uninterrupted double helix which dissociates in an all-or-none process was in fairly good agreement with the width of the transitions and the kinetic data [4]. The thermodynamic calculations in the present study, however, show, that the earlier model leads to a major discrepancy between the calculated and measured T_m-values. The model of a defective double helix (Table 2), deduced from this work, is a refinement of our former model. The calculations are based on a completely linear arrangement of the helical sections. However, very few branched hairpins as indicated in Table 2 in the form of dashed hairpins, cannot be excluded. There are independent experimental indications for the presence of internal loops. Gross and his colleagues found that chemical modification of viroids is much more efficient than would be expected without helical defects. Enzymatic digestion with different types of RNases under

Table 2

Physical Properties of the Defective Helix				
Viroid	T_m [°C]	ΔH_{app} $\left[\frac{kJ}{mol}\left(\frac{kcal}{mol}\right)\right]$	G:C cont. [%]	Number of base pairs (estim. fr. sta- tist. analysis)
CPFV	51 ±0.2	3470±160 (830)	65±2	86 ±4
PSTV	51 ±0.2	3770±190 (900)	66±2	94 ±5
CEV	51 ±0.2	3390±160 (810)	65±2	84 ±4
ChSTV	48.5±0.2	3160±270 (750)	59±4	78 ±7
ChCMV	48.5±0.2	3160±160 (750)	59±3	78 ±4

limiting conditions confirms the above (Gross, H.J., in prepara-
tion, [26]).

   We have estimated in our present work, that each helical se-
quence of 4-5 base pairs is followed by a defect on the average
in form of an internal loop of two bases. These two parameters,
namely, the mean number of base pairs in one helical section, and
the mean size of the internal loop cannot be separately evaluated
on the basis of their thermodynamic behaviour. As can be seen
clearly from Table 1, longer helical sequences may be compensated
by larger internal loops leading to similar values of T_m and of
the cooperativity. The thermodynamic properties of viroids are
similar to mismatched synthetic polynucleotides in which high co-
operativity is combined with low T_m-values [27,28]. To our
knowledge, viroids are the first example of such a thermodynamic
behaviour which has been found in nature, to date.
The high cooperativity is not very sensitive to a particular
choice of model parameters. It is evident from the results, main-
ly from Table 1, that it is the T_m-value, which is sensitive to
the data from oligonucleotides via the helical length, internal
loop size and G:C content, whereas the cooperativity is only
little affected. The physical basis of the high cooperativity is
the circularity and the low ratio of nucleation parameter/growth
parameter due to the low T_m-value. The cooperativity is also not

seriously lowered by a certain amount of inhomogeneity in the
size of helices and internal loops and the G:C content. A longer
helix may be compensated by a larger loop. An obvious criterium
is that a single helical section, if all other base pairs were
dissociated, may not melt at higher temperature than T_m of the
cooperative transition. It follows straightforward from the
oligonucleotide parameters that in viroids no helical section
with more than about 10 base pairs of 50% G:C or 8 base pairs of
75% G:C will be found. It has been assumed above, that A:U and
G:C base pairs will not exist in clusters. This assumption has
not to hold for each helical section. For example, a pure AU
helical section of 4-5 base pairs right next to a pure GC helical
section would not destroy the cooperativity. Considering several
neighboured helical sections, however, AU and GC pairs will be
distributed fairly homogenous over the whole molecule.

2. Number of base pairs

The generalized thermodynamic model of viroids allows a more
correct estimation of the number of base pairs than the all-or-
none model did, because the cooperativity can be taken into ac-
count quantitatively. Although it was not possible to calculate
the cooperativity of a defective double helix of the actual size
of viroids, values near 85% were extrapolated from the one-heli-
cal-sequence model as well as for defective double helices. The
final gap between the cooperativity of model RNA molecules and
the cooperativity of viroids is filled exactly by a comparison
with the calorimetric results (see accompanying paper [7]).
Taking into account an extrapolated cooperativity of 85% a total
reaction enthalpy of 3,990 kJ/mol for CEV (Table 2) is calculated
from the optical measurements, which is in agreement with 4,200
kJ/mol, obtained by calorimetry.

An estimation of the numbers of base pairs N is listed in
Table 2. These numbers are calculated according to $N = \Delta H_{app}/$
$(\Delta H_{bp} \cdot Cooperativity)$ with an average ΔH_{bp} of 47.3 kJ/mol for
$T_m = 76^\circ C$ and ~65% GC. The accuracy of N is limited for the fol-
lowing reasons. Elementary parameters of other authors [11,12]
would lead to 5-10% higher numbers of N. The main uncertainties
are the enthalpic contributions of the base pairs adjacent to
the unpaired but possibly stacked bases inside the loops. In one

extreme (no enthalpic contribution of the first base pair of a helical section) 10-20 base pairs would have to be added, in the other extreme (high stacking interaction in the internal loop) about the same number would have to be subtracted.

It was further concluded that the size of helical sections and the size of the neighboured internal loops are correlated (cf. Table 1). Combinations of 4 base pairs and 2-4 unpaired bases, or 5 base pairs and 5-7 unpaired bases, 6 base pairs and 7-9 unpaired bases, etc. are in accordance with the experimental and theoretical results. Summing up the paired and looped regions results in 250-300 nucleotides. This means that we need 250-300 out of total 350 nucleotides to interpret the thermodynamic behaviour of viroids. In consequence, the structure denaturing during the melting process (cf. Fig. 1) comprises the major part of the molecule. Whereas in our earlier study on CPFV [4] we evaluated separately the slow and the fast denaturation processes and noted that this procedure was only an approximation we were able in this study to give a general thermodynamic description of the sum of both processes occurring in viroids.

*to whom correspondence should be addressed

+ present address: Stanford University, School of Medicine, Dept. of Biochemistry, Stanford, Calif. 94305

**Arbeitsgruppe Pflanzenvirologie, Justus-Liebig -Universität, Schubertstr. 1, D 6300 Giessen, GFR

REFERENCES

1 Diener, T.O. (1974), Ann. Rev. Microbiol. 28, 23-39
2 Sänger, H.L., Klotz, G., Riesner, D., Gross, H., and Kleinschmidt, A.K. (1976), Proc. Nat. Acad. Sci. USA 73, 11, 3852-3856
3 Semancik, J.S., Morris, T.I., Weathers, L.G., Rodorf, B.F., and Kearns, D.R. (1975), Virology 63, 160-167

4 Henco, K., Riesner, D., and Sänger, H.L. (1977), Nucl.
   Acids Res. 4, 1, 177-194
5 Gross, H.J., Domdey, H., and Sänger, H.L. (1977), Nucl.
   Acids Res. 4, 6, 2021-2028
6 CPFV : cucumber pale fruit viroid
   CEV : citrus exocortis viroid
   PSTV : potato spindle tuber viroid
   ChCMV: chrysanthemum chlorotic mottle viroid
   ChSTV: chrysanthemum stunt viroid
7 Klump, H., Riesner, D., and Sänger, H.L., (1978), Nucleic Acids Res. 5,
   1581-1587
8 Singh, A. and Sänger, H.L. (1976), Phytopath. Z. 87,
   143-160
9 Coutts, S.M., Riesner, D., Römer, R., Rabl, C.R., and
   Maass, G. (1975), Biophys. Chem. 3, 275-289
10 Riesner, D. and Römer, R. (1973) In: "Physico-chemical Pro-
   perties of Nucleic Acids" (J. Duchesne, ed.) Vol. II.,
   pp 237-318, Academic Press, London and New York
11 Borer, P.N., Dengler, B., Tinoco jr., I., and Uhlenbeck,O.C.
   (1974), J. Mol. Biol. 86, 843-853
12 Gralla, J. and Crothers, D.M. (1973), J. Mol. Biol. 73,
   497-511
13 Pörschke, D., Uhlenbeck, O.C., and Martin, F.H. (1973),
   Biopolymers 12, 1313-1335
14 Kallenbach, N.R. (1968), J. Mol. Biol. 37, 445-466
15 Elson, E.L., Scheffler, I.E., and Baldwin, R.L. (1970),
   J. Mol. Biol. 54, 401-415
16 Jacobson, H. and Stockmayer, J. (1950), J. Chem. Phys. 18,
   1600-1606
17 Inners, L.D. and Felsenfeld, G. (1970), J. Mol. Biol. 50,
   373-389
18 DeLisi, C. and Crothers, D.M. (1971), Biopolymers 10,
   2323-2343
19 Rubin, H. and Kallenbach, N.R. (1975), J. Chem. Phys. 62,
   7, 2766-2776
20 Gralla, J. and Crothers, D.M. (1973), J. Mol. Biol. 78,
   301-319
21 Scheffler, I.E., Elson, E.L., and Baldwin, R.L. (1970),
   J. Mol. Biol. 48, 145-171
22 Langowski, J. (1976), Diplomarbeit, Technische Universität
   Hannover
23 Holder, J.W. and Lingzel, J.B. (1975), Biochemistry 14,
   4209-4215
24 Van, N.T., Holder, J.W., Woo, S.L.C., Means, A.R., and
   O'Malley, B.W. (1976), Biochemistry 15, 2054-2062
25 Cox, R.A. (1970), Biochem. J. 117, 101-118
26 Dickson, E., Prensky, W., and Robertson, H.D. (1975),
   Virology 68, 309-316
27 Lomant, A.J. and Fresco, J.R. (1973), Biopolymers 12,
   1889-1903
28 Dodgson, J.B. and Wells, R.D. (1977), Biochemistry 16,
   2367-2374
29 Applequist,J. (1967), In "Conformations of Biopolymers"
   (G.N. Ramachandran, ed.), p.403-425. Acdemic Press,
   New York and London.
30 Pörschke, D. (1968), Thesis, Technische Universität
   Braunschweig